J Appl Electrochem (2014) 44:233–243
DOI 10.1007/s10800-013-0635-1

RESEARCH ARTICLE

Electrochemical investigation of Pd nanoparticles and MWCNTs supported Pd nanoparticles-coated electrodes for alcohols (C_1–C_3) oxidation in fuel cells

Meissam Noroozifar · M. Khorasani-Motlagh · M.-S. Ekrami-Kakhki · R. Khaleghian-Moghadam

Received: 24 June 2013 / Accepted: 7 October 2013 / Published online: 17 October 2013

Abstract Incorporation of palladium nanoparticles (Pd NPs) and multi-walled carbon nanotubes (MWCNTs) into chitosan-coated glassy carbon (GC) electrode for alcohols (methanol, ethanol, and isopropanol) electrooxidation has been studied. PdNPs–chitosan and MWCNTs–PdNPs–chitosan nanocomposites are successfully prepared and characterized by transmission electron microscopy images and UV–Vis spectroscopy. Based on the results, PdNPs–chitosan nanocomposite indicates high electrochemical activity and excellent catalytic characteristic for alcohol (C_1–C_3) electrooxidation on a GC electrode in an alkaline medium. The current density of the alcohols oxidation at GC–PdNPs–chitosan electrode is investigated in optimized conditions and compared with that obtained at the GC-modified electrode by Pd with different polymers. Also, our results show that the dispersion of Pd nanoparticles on the MWCNTs significantly improved the performance of the PdNPs/chitosan composite for electrooxidation of the C_1–C_3 alcohols.

Keywords Palladium · Chitosan · MWCNTs · Nanoparticles · Fuel cell · Electrocatalyst

1 Introduction

Electrooxidation of alcohols especially methanol, ethanol, and isopropanol has been investigated extensively because of their great potential in energy-saving technologies such as direct alcohol fuel cells (DAFCs) [1, 2]. The interest in the development of DAFCs has lead to the intense researches about the catalytic materials for the electrooxidation of alcohols. Pt-based catalysts are considered to have the best catalytic activity for low-temperature fuel cells [3] but, their high cost and limited resource of Pt [4] restricted their use. Up to date, many investigations have been performed for the electro-oxidation of alcohols on DAFCs in acidic media with Pt-based electrocatalysts [5, 6]. Recently, Pd-based catalysts have been studied intensively because of their high activity for the electrooxidation of alcohols in alkaline media where many non-noble metals are stable for electrochemical applications [7–9]. Pd catalysts are much cheaper than Pt-based catalysts and have some potential advantages in DAFCs applications [10, 11]. Furthermore, Pd is at least fifty times more abundant than Pt on the earth, which increases the interest for intensive researches of palladium nanoparticles (PdNPs) in areas of catalysis [12–15]. Also, a suitable catalyst support can increase the catalytic activity and reduce the use of noble metal catalysts.

The preparation of new organic/inorganic hybrid materials and nanocomposites is very important and has been studied numerously [16]. Polymers are considered as a good host material for metals [17–19]. Among many polymer electrolyte membranes studied, chitosan membranes have a better performance for low-temperature fuel cells applications [20]. High sorption capacities, stability of metal anions (such as Pt and Pd) on chitosan, and physical (and chemical) versatility of the biopolymer have made chitosan an interesting support for catalytic metals. Chitosan is an optically active biopolymer that is characterized by a strong affinity for transition metals.

Carbon nanotubes (CNTs) are cylindrical carbon molecules, with at least one end typically capped with a

M. Noroozifar (✉) · M. Khorasani-Motlagh · M.-S. Ekrami-Kakhki · R. Khaleghian-Moghadam
Department of Chemistry, University of Sistan and Baluchestan, P.O. Box 98155-147, Zahedan, Iran
e-mail: mnoroozifar@chem.usb.ac.ir

hemisphere of the buckyball structure. CNTs have special properties, such as high electrical conductivity, chemical stability, and catalyst support, which are useful for catalytic process. Also, they exhibit extraordinary strength and unique electrical properties. CNTs are efficient conductors of heat that make them potentially useful in a wide variety of applications such as nano-electronics and materials applications. The CNT-modified electrodes promote electron transfer due to their conductivity and mechanical properties [21, 22]. Different types of Pd nanocatalyst such as nanoporous palladium rods [23], Raney-like nanoporous Pd [24], and CNTs-supported binary and ternary Pd-based catalysts [25] have been used extensively for electrocatalytic oxidation of methanol, ethanol and methanol, ethanol and formic acid, respectively. To the best of our knowledge, no PdNPs–chitosan and Pd-multi-walled carbon nanotubes (MWCNTs)–chitosan nanocomposite electrodes have been reported for alcohols oxidation.

In this study, the electrooxidation of methanol, ethanol, and isopropanol on the modified glassy carbon (GC) with PdNPs–chitosan and Pd–MWCNTs–chitosan nanocomposite electrodes has been studied in alkaline solution. The electrochemical activity of PdNPs–chitosan nanocomposites toward alcohol (C_1–C_3) oxidation were measured by cyclic voltammetry (CV) and chronoamperometry. The effect of various factors such as scan rate, anodic limit of potentials, concentration of sodium hydroxide, methanol, ethanol, isopropanol, and Pd nanoparticles amounts on the anodic current density and potential of alcohols (C_1–C_3) oxidation was studied and optimum value for each factor was suggested. Also, the electrochemical activity of PdNPs–MWCNTs–chitosan nanocomposites toward alcohol (C_1–C_3) oxidation were measured by CV and compared with nanocomposites without MWCNTs (PdNPs–chitosan).

2 Experimental

2.1 Materials

Chitosan ([2-amino-2-deoxy-(1-4)-β-D-glucopyranose]), with medium molecular weight, 400,000 Da, was purchased from Fluka. MWCNTs with nanotube diameters, OD = 20–30 nm, wall thickness = 1–2 nm, length = 0.5–2 μm, and purity >95 % was purchased from Aldrich. $PdCl_2$ and $NaBH_4$ were purchased from Merck and used without further purification. Acetic acid was diluted to a 1 % aqueous solution before use. Methanol, ethanol, and isopropanol were purchased from Merck. All solutions were prepared by doubly distilled water. Purified N_2 (99.9 %) was used without further treatment.

2.2 Characterization methods

UV–Vis spectra were recorded on an analytikjena SPECORD S100 spectrometer with photodiode array detector. Transmission electron microscopy (TEM) images were taken using a Philips CM120 transmission electron microscope with resolution 2.5 Å.

2.3 Preparation of PdNPs–chitosan nanocomposites

A solution of chitosan (2 mg/mL) in 1 % acetic acid solution was prepared, because of the poor solubility of chitosan; the mixture was stirred to completely dissolve and kept for overnight. Then the solution was filtrated through 0.22-m Millipore syringe filters to remove any impurity before use. Preparation of metal–chitosan nanocomposites is very simple; at first $PdCl_2$ solution (2.0 M) was prepared by dissolving $PdCl_2$ powder in concentrated HCl to form $[PdCl_4]^{2-}$, and the excess HCl was evaporated off at 70 °C in a water bath [26]. Then a 25 μL $PdCl_2$ solution (2.0 M) was mixed with 3 mL chitosan 1 (wt%), the mixtures were stirred in a rotary (rpm 100) for 30 min. The freshly prepared aqueous solution of $NaBH_4$ (50 μL, 5 M) was added quickly to the mixture as the reducing agent and stirred for another 90 min to reduce the metal salts entirely. The resulted nanocomposites (1.62×10^{-2} M of PdNPs) were kept at room temperature for characterization.

2.4 Preparation of MWCNTs–PdNPs–chitosan nanocomposites

MWCNTs were first subjected to the oxidative pretreatment by vigorously stirring in a mixture of concentrated sulfuric acid and nitric acid with the volumetric ratio of 3:1 at room temperature for 24 h. This pretreatment removes impurities and generates sufficient functional groups on the surface of MWCNTs. The treated MWCNTs were filtered by centrifugation (2,000 rpm) and washed with double-distilled water until the pH of the filtrate reached 7. In order to produce PdNPs, metal salts were chemically reduced to their zero valences using $NaBH_4$. To reach complete reduction level, the concentration of $NaBH_4$ was several times of the concentration of the metal salt. The procedure was as follows: 1.5 mg of the functionalized MWCNTs was dispersed into the appropriate amount of 1 % chitosan solution using an ultrasonic bath to obtain a uniform carbon ink. A 25 μL $PdCl_2$ solution (2.0 M) was mixed with a known amount of 1 % chitosan solution using a rotary (100 rpm) for 30 min. The prepared carbon ink was added to the Pd–chitosan mixture and stirred for another 30 min. Then, 50 μL of freshly prepared aqueous solution of 2.5 M $NaBH_4$ was added to the mixture. The mixture was kept

stirring for 90 min to achieve the entire reduction of Pd nanoparticles. The resulting suspension was kept at room temperature for consecutive investigations.

2.5 Electrodes preparation

The GC working electrode with 2 mm of diameter (0.0314 cm^2) was polished with 0.05 μm alumina slurry to a mirror-finish. After sonicating in water and absolute ethanol in an ultrasonic bath for about 5 min each, it was washed with double-distilled water. Next, the GC electrode was cleaned and activated in the electrochemical cell by using CV between −1.5 and +1.5 V at a scan rate of 50 m V s^{-1} in freshly prepared deoxygenated 1.0 mol L^{-1} H_2SO_4 until a stable cyclic voltammetric profile (≈15 times) was obtained and then was used. The suspension of nanocomposites catalyst (PdNPs–chitosan or PdNPs–MWCNTs–chitosan) was spread by pipette onto the surface of the GC electrode. The catalyst layer was formed by evaporation of the solvent.

2.6 Electrochemical studies

Electrochemical measurements have been done in a standard three-electrode cell using an SAMA500 Electroanalyser (SAMA Research Center, Iran). The counter and reference electrodes were platinum and Hg/HgO electrodes, respectively. All potentials were reported according to the reference electrode. Nitrogen bubbling was used to deoxygenate the electrolyte solutions before each voltammetric experiment. The experiments were done under nitrogen atmosphere and the scan rate of 50 mV s^{-1} at room temperature.

3 Results and discussion

3.1 PdNPs–chitosan and MWCNTs–PdNPs–chitosan nanocomposites characterization

Chitosan is an oxygen-rich natural carbohydrate (polysaccharide) containing anhydroglucose units joined by an oxygen linkage to form a linear molecular chain. Pt and Pd nanoparticles could be stabilized and dispersed within chitosan prior to the metal reduction with formations of coordination bonds between the metal ions and amino or hydroxyl groups of chitosan. The theory and experimental data on formation of coordination bonds between metal ions and chitosan have been reported [27, 28]. The formation of metal nanoparticles was confirmed by UV–Vis spectra and TEM observations. The UV–Vis spectrum of palladium–chitosan nanocomposite is shown in Fig. 1. As seen in Fig. 1a, a strong absorption bond at 236 nm is corresponded to the absorption of $PdCl_4^{2-}$ [2, 8]. The UV–Vis spectrum of Pd–chitosan nanocomposite is shown in Fig. 1b. The absorption peak at 236 nm disappeared completely, indicating that Pd(II) has been used up and colloidal Pd has been formed [29]. Based on Fig. 1b, for PdNPs, no plasmon absorbance could be observed. For the colloidal metallic Pd, there is only a continuous absorption in the visible range, rising to broad and poorly resolved absorption bands in the ultraviolet near 200 nm. The difference in the way that the spectra of colloidal particles of different metals change when the particle shape is varied from spherical to spheroidal is investigated systematically in the dipole approximation. The observed spectra are similar to that reported in literature for PdNPs [30].

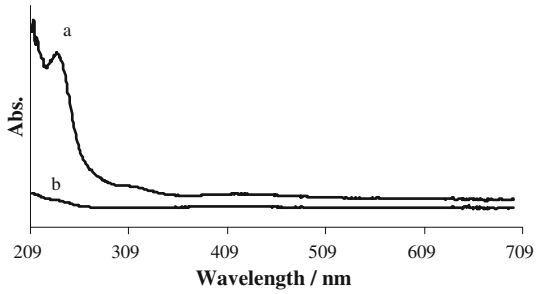

Fig. 1 UV–Vis spectra of (*a*) $PdCl_4^{2-}$ and (*b*) prepared Pd–chitosan nanocomposites

TEM images of MWCNTs–PdNPs and PdNPs in chitosan are shown in Fig. 2a, b. It is seen from Fig. 2b that the overall size of the Pd nanoparticles in chitosan ranges from 5 to 8 nm. It is clear that the use of chitosan allows a better dispersion of nanoparticles through larger portion of the surface and thus prevents agglomeration of metallic particles. Figure 2a illustrates TEM of MWCNTs–PdNPs in chitosan which shows the better dispersion of the catalyst nanoparticles. The size of Pd nanoparticles on MWCNTs–PdNPs ranges from 4 to 6 nm.

X-ray diffraction pattern of the synthesized MWCNTs–PdNPs is shown in Fig. 2c. The XRD pattern confirms the formation of PdNPs on MWCNTs with a main diffraction peak. The strong diffraction peaks at $2\theta = 26.5°$ and 42.4° (inset Fig. 2c) are attributed to MWCNTs (0 0 2) and (1 0 0) planes, respectively. The characteristic peaks at $2\theta = 39.7°$, 46.2°, 67.4°, and 81.2° can be assigned to Pd (1 1 1), (2 0 0), (2 2 0), and (3 1 1) plane, respectively, suggesting that the face-centered cubic palladium was successfully deposited on MWCNTs.

3.2 Electrochemically active surface area of the GC/MWCNTs–PdNPs–CH electrode

The electrochemical active surface area (EASA) was estimated by CV experiments in alkaline solution (NaOH

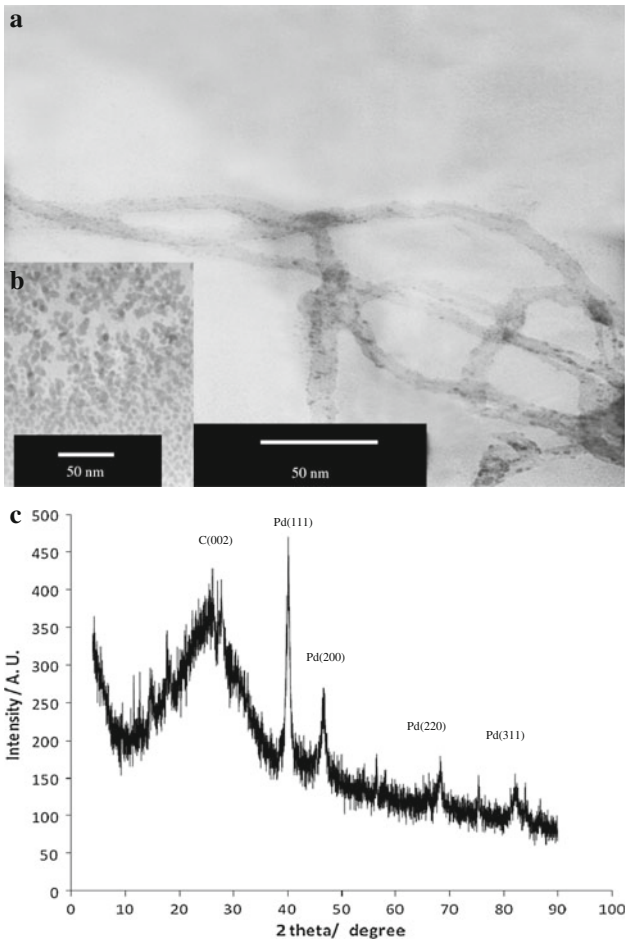

Fig. 2 Typical TEM images of **a** MWCNTs–PdNPs–chitosan nanocomposites and **b** PdNPs–chitosan; and **c** powder XRD patterns of MWCNTs–PdNPs catalyst

1.0 M solution at room temperature). Figure 3 shows the CV curves of the as-prepared catalysts in 1.0 M NaOH solution in the potential range of −0.9 to 0.6 V (vs. Hg/HgO). When the electrode potential is ramped linearly to a more positive potential (with respect to Hg/HgO), protons and electrons are produced from the oxidation of the adsorbed hydrogen on Pd surface and the anodic peak at $E = -0.294$ V is obtained because of the desorption of hydrogen from the electrode surface

$$\mathrm{Pd{-}H_{abs/ads}} + \mathrm{OH^-} \rightarrow \mathrm{Pd} + \mathrm{H_2O} + \mathrm{e^-}. \quad (1)$$

While at higher potential, palladium oxide is produced from Pd nanoparticles. The peak in the potential region from −0.502 V vs. Hg/HgO is attributed to the hydrogen adsorption, when the electrode potential is ramped to a more positive potential, linearly. Similar voltammogram of Pd supported on carbon microspheres in 1.0 M KOH has been found by Xu et al. [31]. The EAS is calculated from Eq. (2):

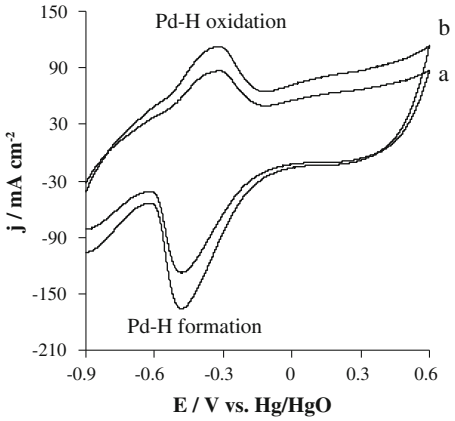

Fig. 3 Cyclic voltammograms of (*a*) PdNPs and (*b*) MWCNTs–PdNPs catalysts in 1.0 M NaOH solution

$$\mathrm{EAS} = \frac{Q_\mathrm{H}}{kL}, \quad (2)$$

where Q_H is the coulombic charge for reduction of palladium oxide; L is the catalyst loading (g) on the electrode, and k is a parameter to relate charge with area; A charge value of 405 μC cm^{-2} is assumed for the reduction of PdO monolayer [32, 33]. The Q_H is 5.47 mC cm^{-2} for MWCNTs–PdNPs with a PdNPs loading of 0.4237 mg cm^{-2}. Whereas, the Q_H is 3.40 mC cm^{-2} for PdNPs film electrode with a PdNPs loading of 1.10 mg cm^{-2}. The EAS of MWCNTs–PdNPs is 4.2 times higher than PdNPs film electrode. The higher EAS of MWCNTs–PdNPs is probably because of the better dispersion and less size of PdNPs [34].

3.3 Electrooxidation of methanol, ethanol, and isopropanol on modified GC with palladium–chitosan nanocomposites

Electrochemical properties of modified GC electrodes with palladium–chitosan nanocomposites toward methanol, ethanol, and isopropanol oxidation have been studied by CV in 0.99 M methanol, 0.55 M ethanol, 0.73 M isopropanol, and 1.0 M NaOH aqueous solution and the typical cyclic voltammograms for GC/chitosan and GC/PdNPs–chitosan are shown in Fig. 4 (CV at GC electrode is not shown, which is similar to that of GC/chitosan electrode). From Fig. 4a, it can be seen that no current peaks of alcohol oxidation can be observed on GC and GC/chitosan electrodes. This indicates that GC and GC/chitosan substrates have no obvious electrocatalytic activity for alcohol (C_1–C_3) oxidation. The cyclic voltammogram for methanol electrooxidation obtained on GC/chitosan electrode containing PdNPs-dispersed electrocatalyst (GC/PdNPs–chitosan) is presented in Fig. 4d and high electrocatalytic activity is observed. As seen in Fig. 4d, two peaks of

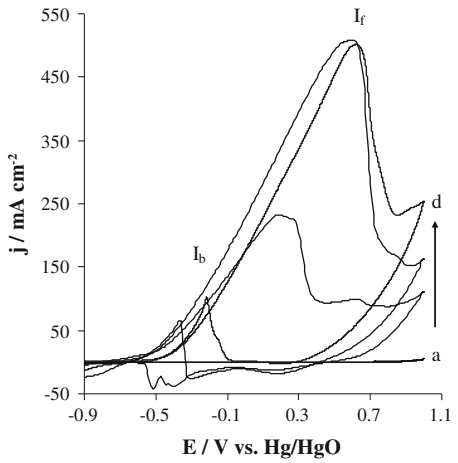

Fig. 4 Cyclic voltammograms in 1.0 M NaOH on (*a*) GC/chitosan in methanol or ethanol or isopropanol, (*b*) GC/PdNPs–chitosan electrodes in 0.73 M isopropanol, (*c*) GC/PdNPs–chitosan electrodes in 0.55 M ethanol, and (*d*) GC/PdNPs–chitosan electrodes in 0.99 M methanol (CV on GC electrode is not shown, which is similar to that of GC–chitosan electrode)

methanol oxidation can be observed obviously in the range of −0.9 to 1.0 V for GC/PdNPs–chitosan electrode. The anodic peak current in the forward scan observed at 0.62 V (E_f) is associated with the oxidation of methanol on Pd. The anodic current peak in the reverse scan at −0.21 V (E_b) is associated with the oxidation of intermediate species adsorbed on Pd [35]. The onset potential of GC/PdNPs–chitosan electrode for methanol electro-oxidation was −0.53 V. I_f/I_b can be used to describe the catalyst tolerance to carbonaceous species accumulation. A low I_f/I_b ratio indicates poor oxidation of alcohols (C_1–C_3) to carbon dioxide during the anodic scan and excessive accumulation of carbonaceous residues on the electrode surface. A high I_f/I_b ratio shows the reverse case [36]. I_f/I_b for methanol oxidation (0.99 M) at GC/PdNPs–chitosan electrode was 5.25. Electrooxidation of ethanol on GC/PdNPs–chitosan electrode is shown in Fig. 4c. As seen in Fig. 4c, 2 oxidation peaks of ethanol oxidation can be observed at 0.6 (E_f) and −0.36 V (E_b). The onset potential of GC/PdNPs–chitosan electrode for ethanol electro-oxidation was −0.64 V. I_f/I_b for ethanol oxidation (0.55 M) at GC/PdNPs–chitosan electrode was 7.86. Electrooxidation of isopropanol on GC/PdNPs–chitosan electrode can be seen in Fig. 4b. As observed in Fig. 4b, two oxidation peaks of isopropanol oxidation can be seen obviously at 0.18 (E_f) and −0.63 V (E_b), respectively. The anodic current density of isopropanol oxidation on GC/PdNPs–chitosan electrode was 232.83 mA cm^{-2} and the onset potential was −0.64 V. The current peak densities (I_f) 501.69, 508.37, and 232.83 mA cm^{-2} and the onset potentials −0.53, −0.64, and −0.64 V were obtained for methanol, ethanol, and isopropanol oxidation, respectively. The characteristics of the CV curves and the corresponding peak potentials (E_p) are in agreement with other works [37–41].

The cyclic voltammograms have been also obtained for the equal and constant concentrations of ethanol, methanol, and isopropanol (0.55 M). In this certain concentration, the current densities (I_f) for ethanol, methanol, and isopropanol oxidation were 508, 467, and 211 mA cm^{-2}, respectively. The anodic peak potential (E_f) for ethanol, methanol, and isopropanol oxidation were observed at 0.60, 0.56, and 0.14 V, respectively. I_f/I_b for ethanol, methanol, and isopropanol at the equal concentration of 0.55 M were 7.85, 6.92, and 4.48, respectively. These results showed that PdNPs–chitosan composite was an electrochemical active catalyst for oxidation of all three alcohols. However, the best performance of GC/PdNPs–chitosan electrode was obtained for ethanol oxidation in terms of the onset potential, I_f/I_b ratio, and the peak current density comparing to other two alcohols.

3.4 Parameters affecting on alcohol electrooxidation

Our primary investigations showed that different parameters such as alcohol (methanol, ethanol, and isopropanol) and palladium concentrations, concentration of sodium hydroxide as the electrolyte, scan rate, and potential were the most important factors influencing the performance of the proposed modified electrode toward alcohols (C_1–C_3) electrooxidation. So, these parameters must be optimized. In addition, the effect of addition of MWCNTs to PdNPs–chitosan on alcohol electrooxidation has been studied.

3.4.1 Effect of alcohol concentration

The effect of alcohol concentration on the anodic current density of alcohol oxidation on the GC/PdNPs–chitosan electrode was studied. It is clearly observed that the anodic current density increases with increasing alcohol concentration. In the case of methanol, the anodic current density levels off at concentrations higher than 0.99 M. Also, when the methanol concentration increases from 0.12 to 0.99 M, the E_f and E_b shift toward positive direction from 0.20 to 0.62 V and −0.71 to −0.22 V, respectively. We assumed that this effect may be due to the saturation of active sites on the surface of the electrode. Also, this indicates further that the electrooxidation of methanol at modified electrode is controlled by diffusion process. In accordance with this result, the optimum concentration of methanol to obtain a higher current density may be considered as about 0.99 M. The effect of ethanol concentration on the anodic current of ethanol oxidation at the GC/PdNPs–chitosan electrode was also investigated. Similarly, when the ethanol concentration increases from 0.06 to 0.55 M, the E_f and E_b shift

Table 1 Electrooxidation of isopropanol on the GC/PdNPs–chitosan electrocatalyst in 1.0 M NaOH

Isopropanol concentration (M)	I_f (mA cm^{-2})	E_f (V)	I_b (mA cm^{-2})	E_b (V)
0.043	51.353	−0.18	–	−0.58
0.086	73.092	−0.12	–	−0.55
0.107	85.729	−0.09	–	−0.53
0.149	105.649	−0.05	–	−0.5
0.192	113.513	−0.03	0.6194	−0.49
0.213	128.545	−0.01	4.746	−0.47
0.275	152.981	0.05	10.423	−0.45
0.296	147.564	0.03	11.476	−0.45
0.337	183.748	0.12	22.539	−0.42
0.358	163.608	0.06	17.689	−0.43
0.399	181.283	0.09	25.198	−0.42
0.419	185.312	0.1	27.686	−0.41
0.459	202.831	0.14	41.073	−0.37
0.499	200.095	0.14	41.392	−0.37
0.539	208.780	0.16	45.701	−0.36
0.579	221.344	0.17	51.376	−0.34
0.598	221.5	0.18	52.083	−0.34
0.638	229.666	0.2	55.169	−0.33
0.677	244.315	0.26	57.478	−0.33
0.697	246.968	0.24	58.379	−0.32
0.716	256.309	0.27	61.191	−0.32
0.730	256.057	0.26	61.169	−0.32

toward positive direction from −0.07 to 0.60 V and −0.67 to −0.36 V, respectively, and the anodic current density of ethanol electrooxidation increases from 113.41 to 508.37 mA cm^{-2}. Table 1 shows the effect of isopropanol concentration on the anodic current density and potential of isopropanol oxidation at GC/PdNPs–chitosan electrode.

For example, Fig. 5 shows the effect of ethanol concentration on the anodic current density of ethanol oxidation on the GC/PdNPs–chitosan electrode.

3.4.2 *Effect of palladium concentration*

The effect of palladium amounts on the anodic current density of methanol oxidation at GC/PdNPs–chitosan electrode was investigated by chronoamperometry in 0.99 M of methanol and 1.0 M NaOH at an anodic potential of 0.8 V vs. Hg/HgO (Fig. 6). In all current–time curves for the GC/PdNPs–chitosan electrodes, there was an initial current drop in the first 9 s followed by a slower decay, but the current values obtained for the GC/PdNPs–chitosan electrocatalysts were always higher than those obtained for GC or GC/chitosan electrocatalysts. The data indicate that the GC–PdNPs–chitosan catalysts have high activity for methanol oxidation as a pure GC and GC/chitosan sample yields zero current from the oxidation. The best result was obtained for electrode of palladium with 16.2 mM compositions.

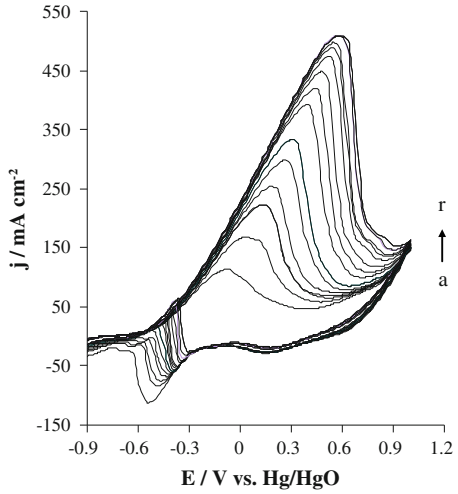

Fig. 5 Cyclic voltammograms for ethanol oxidation on the GC/PdNPs–chitosan electrocatalyst in 1.0 M NaOH in different concentrations of ethanol: (*a*) 0.057, (*b*) 0.085, (*c*) 0.113, (*d*) 0.142, (*e*) 0.17, (*f*) 0.198, (*g*) 0.226, (*h*) 0.254, (*i*) 0.282, (*j*) 0.309, (*k*) 0.337, (*l*) 0.364, (*m*) 0.392, (*n*) 0.419, (*o*) 0.446, (*p*) 0.474, (*q*) 0.501, and (*r*) 0.550 M

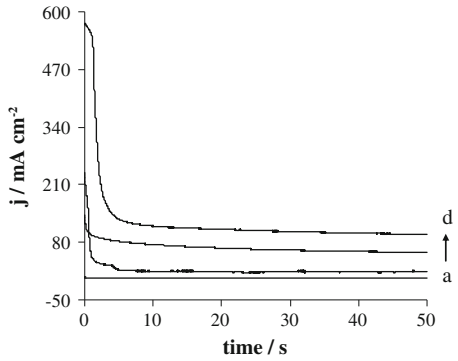

Fig. 6 Chronoamperometry for methanol oxidation on the GC/PdNPs–chitosan electrocatalyst in 1 M NaOH in different concentrations of palladium: (*a*) 0, (*b*) 8.0, (*c*) 26.6, and (*d*) 16.2 mM

3.4.3 *Effect of sodium hydroxide concentration*

Electrooxidation of alcohols (C_1–C_3) were done in different concentrations of NaOH in the range of 0.1–2.0 M. The best result for the same amount of Pd is shown with NaOH 1.0 M. It is probably due to the solubility of chitosan that depends on the pH of the solution. Chitosan is readily soluble in dilute acidic solutions below pH 6.0. This is because chitosan can be considered a strong base as it possesses primary amino groups with a pK_a value of 6.3. The presence of the amino groups indicates that pH substantially alters the charged state and properties of

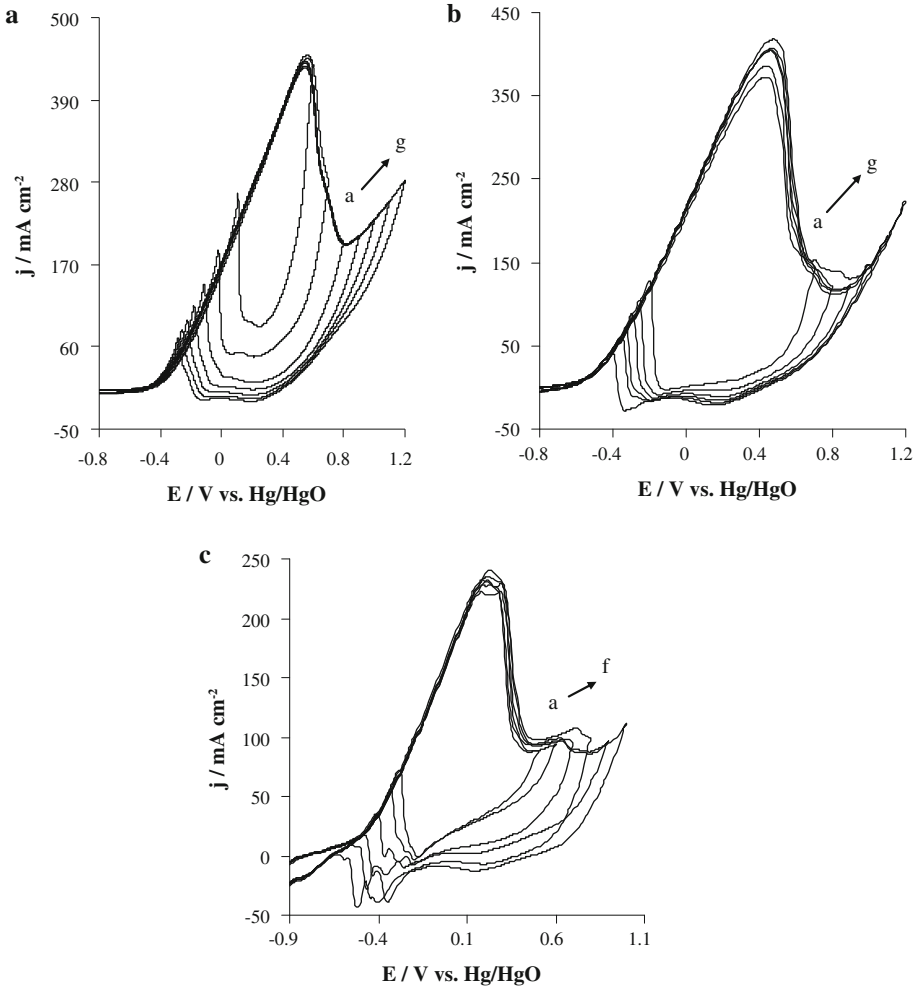

Fig. 7 The effect of limit of potential on **a** methanol (0.99 M), **b** ethanol (0.55 M), and **c** isopropanol (0.73 M) electrooxidation on the GC–PdNPs–chitosan at the same concentration of Pd nanoparticles

chitosan. At low pH, these amines get protonated and become positively charged and that makes chitosan a water-soluble cationic polyelectrolyte. On the other hand, as the pH increases above 6, chitosan's amines become deprotonated and the polymer loses its charge and becomes insoluble. So, chitosan is insoluble in NaOH 1.0 M and the experiments were done in this concentration of sodium hydroxide.

3.4.4 Effect of limit of potential

The effect of anodic limit of potential scanning on the electrooxidation of methanol, ethanol, and isopropanol at GC/PdNPs–chitosan was studied and the cyclic voltammograms were obtained in the conditions that the final potential is varied between 0.6 and 1.2 V for methanol and ethanol and 0.5–1 for isopropanol (Fig. 7). As seen in Fig. 7, for all three alcohols (C_1–C_3) oxidation, with increasing the final potential limit to more positive potentials, E_b and I_b are decreased. When limit of potential scanning increases from 0.6 and 1.2 V, for methanol electrooxidation, I_f/I_b increases from 1.69 to 6.18, and $E_{p(Ib)}$ decreases from 0.11 to −0.28 V; and for ethanol electrooxidation, I_f/I_b increases from 2.40 to 9.08, and $E_{p(Ib)}$ decreases from −0.07 to −0.42 V. It seems that the increase of the limit of potential scanning will decrease the poisoning rate of the Pd catalyst. Probably, by increasing the final positive potentials, the conversion of Pd to PdO is accelerated and causes a decrease in I_b, which further demonstrates that methanol, ethanol, and isopropanol can only be oxidized on clean metallic palladium particles surface [42, 43].

3.4.5 Effect of scan rate

For example, Fig. 8 shows the cyclic voltammograms of methanol oxidation on GC/PdNPs–chitosan electrode in 1 M NaOH solution with different scan rates. As seen in Fig. 8, the peak potential of the forward scan increase with the increase of v. The same results were obtained for ethanol and isopropanol oxidation on GC/PdNPs–chitosan electrode with different scan rates. In all cases, there is a

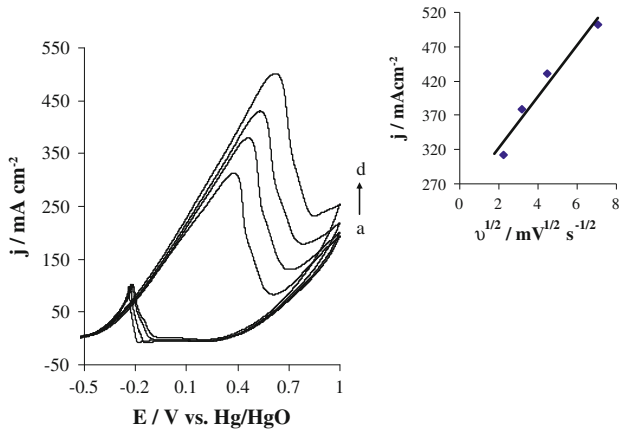

Fig. 8 Effect of scan rate for methanol (0.99 M) electrooxidation on the GC/PdNPs–chitosan with the scan rates of (*a*) 5, (*b*) 10, (*c*) 20, and (*d*) 50 mV s^{-1}

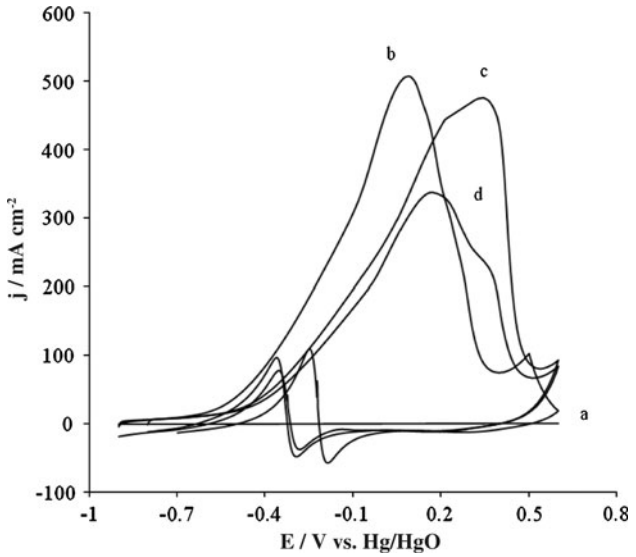

Fig. 9 Cyclic voltammograms in 1.0 M NaOH on (*a*) GC/MWCNTs–chitosan in methanol or ethanol or isopropanol, (*b*) GC/MWCNTs–PdNPs–chitosan electrode in 0.99 M methanol, (*c*) GC/MWCNTs–PdNPs–chitosan electrode in 0.55 M ethanol, and (*d*) GC/MWCNTs–PdNPs–chitosan electrode in 0.73 M isopropanol

linear relationship between the peak current density of the forward CV scan and $v^{1/2}$ (inset of Fig. 8) and reveals that the process of alcohols (methanol, ethanol, and isopropanol) oxidation may be controlled by diffusion of the corresponding alcohols from the bulk solution to the electrode surface [44].

3.4.6 Effect of addition of MWCNTs

To study the effect of MWCNTs on the performance of the electrode, electrooxidation of methanol, ethanol, and isopropanol on modified GC with MWCNTs–PdNPs–chitosan has been studied in optimum condition of the electrode without MWCNTs (methanol 0.99, ethanol 0.55, isopropanol 0.73 M, and NaOH 1.0 M).

The CVs related to methanol oxidation on the GC/MWCNTs–PdNPs–chitosan electrodes are shown in Fig. 9. As seen in Fig. 9(curve a), no current peaks of methanol oxidation can be observed on the GC/MWCNTs–chitosan electrode indicating that this electrode has no obvious electrocatalytic activity toward methanol oxidation. This is because no Pd particles have been deposited on the MWCNTs. Similar results were obtained for the GC and GC/CH electrodes whose corresponding CVs have not been represented. As seen in Fig. 9(curves b), two peaks with considerable current density can be observed in the range of −0.5 to 0.5 V for methanol on the GC/MWCNTs–PdNPs–chitosan electrodes. The peak observed on the forward scan (E_f) at 0.20 V is assigned to the oxidation of methanol. The peak observed on the backward scan (E_b) at −0.36 V is ascribed to the oxidation of the corresponding intermediates produced during the methanol oxidation process.

The CVs related to ethanol and isopropanol oxidation on the GC/MWCNTs–PdNPs–chitosan electrode are studied and shown in Fig. 9c, d.

By comparison of electrochemical data on GC/PdNPs–chitosan (see Fig. 4 and Table 2) and GC/MWCNT–PdNPs–chitosan (see Fig. 9 and Table 2) electrodes, it is clear that by adding MWCNTs to PdNPs, the potential of the E_f and E_b shift considerably toward negative potential for all alcohols. The results showed that the overpotential was reduced with a value of 420, 260, and 80 mV for the oxidation of methanol, ethanol, and isopropanol, respectively. Based on the results, the CNT-modified electrodes promote electron transfer due to their conductivity property. Also, wrapping CNT by polymeric chains is now a new approach for achieving the solubility without any considerable impairment their physical, chemical, and electrochemical properties [45].

As seen in Table 2, there is also an improvement in EASA of Pd electrode with introduction of MWCNTs to the Pd electrode. The results demonstrate that the observed higher EASA of Pd–MWCNTs composite electrodes have been caused due to the modification of both the geometrical and electronic properties of materials. The deposition of PdNPs on MWCNTs most likely takes place at the sulfonic acid functional groups. This avoids the aggregation and non-uniform size distribution of PdNPs on MWCNTs surface. Furthermore, the special frame and properties of Pd–hydrophilic groups–MWCNTs hybrids may facilitate the transmission of the electrolyte and alcohol through the surface of the catalyst [46, 47]. Thus the liquid sealing effect reduces greatly due to the facilitated diffusion of the liquid reactants onto the electrode surface. This would enhance the active surface area for electrochemical reactions.

Table 2 Electrochemical data for alcohol (C_1–C_3) oxidation on GC-modified electrode with various catalysts (reference electrode is Hg/HgO)

Catalyst composition	Onset alcohol oxidation potential (V)	E_f (V)	I_f (mA cm^{-2})	Scan rate (mV s^{-1})	Electrolyte	EASA (m^2 g^{-1})	References
Pd/C–(PTFE)[a]	−0.38	−0.08	24	5	1.0 M CH_3OH + 1.0 M KOH	24	[31]
Pd/C–(PTFE)	−0.52	−0.14	27	5	1.0 M C_2H_5OH + 1.0 M KOH	24	[31]
Pd/CMS[b]–(PTFE)	−0.49	−0.09	50	5	1.0 M CH_3OH + 1.0 M KOH	50	[31]
Pd/CMS–(PTFE)	−0.58	−0.14	65	5	1.0 M C_2H_5OH + 1.0 M KOH	50	[31]
Pd–Nafion	−0.38	−0.06	108.37[c]	50	1.0 M CH_3OH + 1.0 M KOH	10.5	[33]
Pd–5 %MWCNTs–Nafion	−0.55	−0.06	154.17[c]	50	1.0 M CH_3OH + 1.0 M KOH	10.8	[33]
Pd–Nafion	−0.53	−0.14	7.99	50	1.0 M C_2H_5OH + 1.0 M KOH	42.5[d]	[41]
Pd–5 %MWCNTs–Nafion	−0.61	−0.06	67.5	50	1.0 M C_2H_5OH + 1.0 M KOH	41.4[d]	[41]
Commercial Pd/C–(PVP)[e]	−0.47	−0.05	0.8	50	2.0 M CH_3OH + 1.0 M KOH	45.7	[49]
Cuboctahedral Pd/WC–(PVP)[e]	−0.57	−0.13	1.38	50	2.0 M CH_3OH + 1.0 M KOH	22.7	[49]
PdNPs–chitosan	−0.53	0.62	502	50	0.99 M CH_3OH + 1.0 M NaOH	36.5	This work
PdNPs–MWCNT–chitosan	−0.75	0.20	509	50	0.99 M CH_3OH + 1.0 M NaOH	47.7	
PdNPs–chitosan	−0.64	0.60	508	50	0.55 M C_2H_5OH + 1.0 M NaOH	39.5	
PdNPs–MWCNT–chitosan	−0.82	0.34	475	50	0.55 M C_2H_5OH + 1.0 M NaOH	47.7	
PdNPs–chitosan	−0.64	0.26	256	50	0.73 M C_3H_7OH + 1.0 M NaOH	39.5	
PdNPs–MWCNT–chitosan	−0.72	0.18	336	50	0.73 M C_3H_7OH + 1.0 M NaOH	47.7	

[a] Polytetrafluoroethylene, [b] carbon microspheres, [c] mA cm^{-2} mg^{-1}, [d] mC cm^{-2} mg^{-1}, [e] poly (vinyl pyrrolidone)

Based on the oxidation mechanisms for ethanol [30, 48], the mechanism of ethanol oxidation on GC/MWCNTs–PdNPs–CH electrode might be as follows:

$$CH_3CH_2OH + 3OH^- \leftrightarrow CH_3CO_{ads} + 3H_2O + 3e, \quad (3)$$

$$OH^- \leftrightarrow OH_{ads} + e, \quad (4)$$

$$PdNPs + CH_3CH_2OH \rightarrow PdNPs{-}CH_3CO_{ads} + PdNPs{-}H, \quad (5)$$

$$MWCNTs + PdNPs + H_2O \rightarrow MWCNTs{-}OH_{ads} + PdNPs{-}H, \quad (6)$$

$$PdNPs{-}H \rightarrow PdNPs + H^+ + e, \quad (7)$$

$$MWCNTs{-}OH_{ads} + PdNPs{-}CH_3CO_{ads} \rightarrow MWCNTs + PdNPs + CH_3COOH. \quad (8)$$

Selected electrochemical data for alcohols (C_1–C_3) oxidation at GC-modified electrode with various catalysts are listed in Table 2 [31, 33, 41, 49]. The oxidation current density at the GC/PdNPs–chitosan and GC/MWCNTs–PdNPs–chitosan for a fixed concentration of methanol, ethanol, and isopropanol is considerably higher than that obtained at GC-modified electrode by Pd with different polymers such as polytetrafluoroethylene (PTFE), nafion, and poly(vinyl pyrrolidone) (PVP); and different supports such as carbon black, carbon microspheres, and MWCNTs. EASA of the GC/PdNPs–chitosan and GC/MWCNTs–PdNPs–chitosan is also much higher than that mentioned in Table 2, showing their higher catalytic activity toward alcohols (C_1–C_3) oxidation.

4 Conclusions

The aim of this research is to increase the activity of anodic catalysts and to decrease the loading of noble metal in anodes for methanol, ethanol, and isopropanol electrooxidation. In order to decrease the cost of anode materials, we used dispersion of the PdNPs and MWCNTs in chitosan matrix. The GC/PdNPs–chitosan and GC/MWCNTs–PdNPs–chitosan electrodes were synthesized as active electrocatalysts for methanol, ethanol, and isopropanol electrooxidation. The results showed that, the addition of chitosan into Pd catalysts can significantly improve the performance of the electrode for alcohols (C_1–C_3) electrooxidation. Nontoxicity and good adhesion to the electrode substrate are the great advantages of chitosan. The increase of the catalytic activity of the as-prepared electrode toward methanol, ethanol, and isopropanol oxidation may be because of the decrease in the poisoning effect and the possible dispersion of the metallic particles inside the chitosan which gives electrodes with higher surface areas. Also, our results revealed that adding MWCNTs significantly improved the performance of the PdNPs–chitosan nanocomposite for the oxidation of the C_1–C_3 alcohols, especially methanol, and also reduced Pd metal loading in the catalyst. This is due to the high surface area and electrical conductivity of MWCNTs which lead to better dispersion of the catalyst particles and the anodic current density enhancement.

Acknowledgments We thank University of Sistan and Baluchestan (USB) for financial support.

References

1. Vigier F, Coutanceau C, Hahn F, Belgsir EM, Lamy C (2004) J Electroanal Chem 563:81–89
2. Jayashree RS, Spendelow RS, Yeom J, Rastogi J, Shannon MA, Kenis PJA (2005) Electrochim Acta 50:4674–4682
3. Abdel Rahim MA, Hassan HB, Abdel Hameed RM (2007) Fuel Cells 7:298–305
4. Benseba F, Farah AA, Wang DS, Bock C, Du XM, Kung J, Page YL, Girishkumar JG, Vinodgopal K, Kamat PV (2005) J Phys Chem B 109:15339–15344
5. Ekrami-Kakhki MS, Khorasani-Motlagh M, Noroozifar M (2011) J Appl Electrochem 41:527–534
6. Khorasani-Motlagh M, Noroozifar M, Ekrami-Kakhki MS (2011) Int J Hydrogen Energy 36:11554–11563
7. Xu MW, Gao GY, Zhou WJ, Zhang KF, Li HL (2008) J Power Sources 175:217–220
8. Hu FP, Cui GF, Wei ZD, Shen PK (2008) Electrochem Commun 10:1303–1306
9. Bianchini C, Bambagioni V, Filippi J, Marchionni A, Vizza F, Bert P, Tampucci A (2009) Electrochem Commun 11:1077–1080
10. Liang ZX, Zhao TS, Xu JB, Zhu LD (2009) Electrochim Acta 54:2203–2208
11. Zhang LL, Lu TH, Bao JC, Tang YW, Li C (2006) Electrochem Commun 8:1625–1627
12. Ranganathan ES, Bej SK, Thompson LT (2005) Appl Catal A 289:153–162
13. Wang J, Chen Y, Liu H, Li R, Sun X (2010) Electrochem Commun 12:219–222
14. Savadogo O, Lee K, Oishi K, Mitsushima S, Kamiya N, Ota KI (2004) Electrochem Commun 6:105–109
15. Zhang KF, Guo DJ, Liu X, Li J, Li HL, Su ZX (2006) J Power Sources 162:1077–1081
16. Mark JE (1996) Polym Eng Sci 36:2905–2920
17. Akamatsu K, Takei S, Mizuhata M, Kajinami A, Deki S, Takeoka S, Fujii M, Hayashi S, Yamamoto K (2000) Thin Solid Films 359:55–60
18. Zeng R, Rong MZ, Zhang MQ, Liang HC, Zeng HM (2002) Appl Surf Sci 187:239–247
19. Cole DH, Shull KR, Baldo P, Rehn L (1999) Macromolecules 32:771–779
20. Osifo PO, Masala AJ (2010) J Power Sources 195:4915–4922
21. Tong H, Li HL, Zhang XG (2007) Carbon 45:2424–2432
22. Baughman RH, Zakhidov A, de Heer WA (2002) Science 297:787–792
23. Wang X, Wang W, Qi Z, Zhao C, Ji H, Zhang Z (2010) J Power Sources 195:6740–6747
24. Wang X, Wang W, Qi Z, Zhao C, Ji H, Zhang Z (2012) Int J Hydrogen Energy 37:2579–2587
25. Zhu F, Ma G, Bai Z, Hang R, Tang B, Zhang Z, Wang X (2013) J Power Sources 242:610–620

26. Cotton FA, Wilkinson G, Gaus PL (1987) Basic inorganic chemistry, 2nd edn. Wiley, Singapore, p 536
27. Micera G, Deiana S, Dessi A, Decock P, Dubois D, Kozlowski H (1985) Inorg Chim Acta 107:45–48
28. Guibal E, Sweeney NVO, Zikan MC, Vincent T, Tobin JM (2001) Int J Biol Macromol 28:401–408
29. Morin MC, Lamy C, Léger JM, Vasquez JL, Aldaz A (1990) J Electroanal Chem 283:287–302
30. Creighton JA, Eadon DG (1991) J Chem Soc Faraday Trans 87:3881–3891
31. Xu C, Cheng L, Shen P, Liu Y (2007) Electrochem Commun 9:997–1001
32. Pattabiraman R (1997) Appl Catal A 153:9–20
33. Singh RN, Singh A, Anindita (2009) Int J Hydrogen Energy 34:2052–2057
34. Wang H, Xu C, Cheng F, Jiang S (2007) Electrochem Commun 9:1212–1216
35. Sanmant PV, Fernandes JB, Rangel CM, Figueiredo JL (2005) Catal Today 102–103:173–176
36. Zhao GY, Xu CL, Guo DJ, Li H, Li HL (2006) J Power Sources 162:492–496
37. Sun ZP, Zhang XG, Liu RL, Liang YY, Li HL (2008) J Power Sources 185:801–806
38. Yan Z, Meng H, Shi L, Li Z, Shen PK (2010) Electrochem Commun 12:689–692
39. Wang X, Hu C, Xiong Y, Liu H, Du G, He X (2011) J Power Sources 196:1904–1908
40. Yan Z, He G, Zhang G, Meng H, Shen PK (2010) Int J Hydrogen Energy 35:3263–3269
41. Singh RN, Singh A, Anindita (2009) Carbon 47:271–278
42. Hu CC, Liu KY (1999) Electrochim Acta 44:2727–2738
43. Nozad AG, Ghannadi MM, Sedaghat SS, Taghi-Ganji KM, Yari M (2006) Electroanalysis 18:911–917
44. Honda K, Yoshimura M, Rao TN, Tryk DA, Fujishima A, Yasui K, Sakamoto Y, Nishio K, Masuda H (2001) J Electroanal Chem 514:35–40
45. O'Connell MJ, Poul P, Ericson LM, Huffman C, Wang Y, Haroz E, Kuper C, Tour J, Ausman KD, Smalley RE (2001) Chem Phys Lett 342:265–271
46. Yang W, Wang XL, Yang F, Yang C, Yang XR (2008) Adv Mater 9999:1–9
47. Wen ZH, Wang Q, Li JH (2008) Adv Funct Mater 18:959–964
48. Kua J, Goddard WA (1999) J Am Chem Soc 121:10928–10941
49. Lee YW, Ko AR, Han SB, Kim HS, Kim DY, Kim SJ, Park KW (2010) Chem Commun 46:9241–9243